energies

MDPI

Article

Integrated Operational Planning of Battery Storage Systems for Improved Efficiency in Residential Community Energy Management Using Multistage Stochastic Dual Dynamic Programming: A Finnish Case Study

Pattanun Chanpiwat [1,2,*], Fabricio Oliveira [3] and Steven A. Gabriel [3,4,5]

[1] Department of Graduate Studies, Command and General Staff College, Royal Thai Army, 820/1 Rama V Rd., Nakhon-Chai-Si Road, Dusit, Bangkok 10300, Thailand
[2] Department of Civil Engineering, Chulachomklao Royal Military Academy, Nakhon Nayok 26001, Thailand
[3] Department Mathematics and Systems Analysis, School of Science, Aalto University, FI-00076 Espoo, Finland; fabricio.oliveira@aalto.fi (F.O.); sgabriel@umd.edu (S.A.G.)
[4] Applied Mathematics & Statistics, and Scientific Computation Program, Department of Mechanical Engineering, University of Maryland, College Park, MD 20742, USA
[5] Department of Industrial Economics and Technology Management, Norwegian University of Science and Technology, NO-7491 Trondheim, Norway
* Correspondence: pattanun.chanpiwat@gmail.com

Abstract

This study introduces a novel approach for optimizing residential energy systems by combining linear policy graphs with stochastic dual dynamic programming (SDDP) algorithms. Our method optimizes residential solar power generation and battery storage systems, reducing costs through strategic charging and discharging patterns. Using stylized test data, we evaluate battery storage optimization strategies by comparing various SDDP model configurations against a linear programming (LP) benchmark model. The SDDP optimization framework demonstrates robust performance in battery operation management, efficiently handling diverse pricing scenarios while maintaining computational efficiency. Our analysis reveals that the SDDP model achieves positive financial returns with small-scale battery installations, even in scenarios with limited photovoltaic generation capacity. The results confirm both the economic viability and environmental benefits of residential solar–battery systems through two key strategies: aligning battery charging with renewable energy availability and shifting energy consumption away from peak periods. The SDDP framework proves effective in managing battery operations across dynamic pricing scenarios, achieving performance comparable to LP methods while handling uncertainties in PV generation, consumption, and pricing.

Keywords: power grid; stochastic dual dynamic programming; battery storage scheduling; variable renewable energy

Academic Editors: Giovanni Lutzemberger, Don Hur and Minhan Yoon

Received: 14 April 2025
Revised: 17 June 2025
Accepted: 27 June 2025
Published: 6 July 2025

Citation: Chanpiwat, P.; Oliveira, F.; Gabriel, S.A. Integrated Operational Planning of Battery Storage Systems for Improved Efficiency in Residential Community Energy Management Using Multistage Stochastic Dual Dynamic Programming: A Finnish Case Study. *Energies* **2025**, *18*, 3560. https://doi.org/10.3390/en18133560

1. Introduction

Under the Energy Union framework, Finland has developed and implemented the Finland NECP 2024 (Finland's Integrated National Energy and Climate Plan), which outlines comprehensive energy and climate policies. This strategic initiative reflects Finland's dedication to decarbonization efforts, renewable energy expansion, and enhanced energy efficiency measures. The plan specifically addresses the integration of solar power within

the energy supply sector and establishes improved building regulations for residential and service sectors [1].

Our research is conducted as part of the "EasyDR" initiative, which focuses on enabling demand response (DR) through an open-source approach to optimize residential electricity consumption at scale [2]. The project focuses on implementing variable power source integration through cost-effective solutions, leveraging economical components and open-source technologies.

The envisioned battery storage system optimizes residential energy management through strategic energy storage and distribution. During periods of low demand, the system efficiently captures excess energy, including available photovoltaic generation, for subsequent deployment during peak usage periods. This systematic approach enhances operational efficiency by minimizing energy waste, reducing reliance on fossil fuels during peak demand, and maintaining optimal supply-demand equilibrium [3]. The implementation of localized energy distribution protocols reduces transmission losses while ensuring consistent grid performance parameters [4]. Through the strategic alignment of energy management protocols with solar generation patterns and the utilization of residential storage capabilities, households achieve both economic efficiency and contribute to enhanced grid resilience [5].

Our key innovation consists of the development of an advanced optimization model specifically designed to optimize the scheduling of residential battery storage systems. Building on the seminal research of [6], our work utilizes stochastic dual dynamic programming (SDDP). This sophisticated methodology leverages piecewise linear functions to approximate expected-cost-to-go functions in stochastic dynamic programming, effectively addressing the computational challenges of state discretization. The approach generates estimated functions by analyzing dual solutions of an optimization at each stage. Within stochastic, multistage decomposition frameworks, these solutions can be interpreted as Benders cuts.

The model in [6] presents a notable constraint in its underlying assumption of independent random variables for uncertainty assessment. This framework proves inadequate for electricity market analysis, where stochastic processes demonstrate statistical interdependence. Consider how electricity prices and demand patterns display clear temporal and spatial relationships, with demand peaks typically corresponding to price increases [7]. Given these market dynamics, a more sophisticated approach to uncertainty modeling becomes essential. In [8], an enhanced methodology was introduced for handling stagewise-dependent stochastic processes through multistage, minimax stochastic programming problems. Their approach enables random variables at each stage to correlate with those at other stages, representing a significant advancement of the SDDP algorithm as originally presented in [6]. The framework addresses discrete-time, convex, infinite-horizon, and multistage stochastic programming challenges with continuous state and control variables. By representing SDDP problems through a policy graph structure, this methodology enhances our capacity to address multiple interdependencies.

Research Objectives and Contribution

The current research expands upon existing methodologies and makes two significant contributions. Firstly, we created an SDDP model to solve multistage optimization problems by approximating the expected-cost-to-go functions of stochastic dynamic programming with piecewise-linear functions [6] using a policy graph [8]. This model has been successfully developed for residential community energy management, specifically optimizing battery storage systems while accounting for various market variables, including electricity pricing, photovoltaic (PV) generation, and consumption patterns. Secondly, our

methodology employs advanced time-series forecasting techniques, including exponential smoothing, local-level cycle, and seasonal ARIMA (auto-regressive integrated moving average) models, to generate predictions based on historical data [7,9–12]. By integrating these predicted scenarios and their associated probabilities into our SDDP model, we enhance the optimization of battery storage scheduling throughout the planning period.

To establish a performance benchmark, we evaluate our SDDP model against an LP model with perfect foresight capabilities. This comparative analysis yields valuable economic insights and practical recommendations for battery storage deployment, validated through our empirical testing framework.

This paper is structured as follows: Section 2 introduces the methodological framework, followed by the study data overview in Section 2.1. Section 2.2 addresses uncertainty prediction, while Section 2.3 presents the Linear Policy Graph Model elements. Model assumptions are detailed in Section 2.4. Section 2.5 examines the sub-problems, and Section 2.6 describes the SDDP and LP algorithms. Our empirical findings—including the evaluation of battery storage effectiveness and comparison of stochastic solutions between SDDP and LP models—are presented in Section 3. Section 4 presents our key findings and insights.

2. SDDP and LP Models

In our implementation, the SDDP model leverages piecewise-linear convex functions to estimate expected-cost-to-go functions within the stochastic multistage dynamic programming framework [6]. Piecewise-linear convex functions represent the optimal value functions due to the linear programming formulation of our SDDP subproblem, which is discussed in Section 2.5. Our implementation incorporates a policy graph framework for strategic decision-making, following the methodology outlined by [8]. This approach has demonstrated capability in managing complex uncertainties within multistage optimization [13,14].

2.1. Data

For our complete dataset, we combined German PV generation and demand data obtained from the Collaborating Smart Solar-Powered Microgrids (CoSSMic) initiative [15], along with Finnish day-ahead pricing data from the European Network of Transmission System Operators for Electricity (ENTSO-E) [16]. The CoSSMic dataset, gathered from 1 April to 31 May 2016, encompasses hourly measurements from six households, with four featuring PV generation capabilities. To establish a representative sample of a Finnish housing association, we employed bootstrapping techniques to scale the dataset to 50 households while maintaining the integrity of temporal patterns in both consumption and PV generation. It should be noted that Finnish housing associations function as business entities with centralized management, where both operational costs and financial returns are distributed proportionally among shareholders (i.e., house owners). The ENTSO-E price data covers the period from 1 May 2023, to 1 August 2023. We aligned the 2016 residential energy data with the corresponding 2023 spot market day-ahead pricing timeframe, matching months and weekdays to ensure analytical consistency. Solar radiation patterns between Finland and Germany demonstrate notable similarities, with recorded annual sunlight hours of 1679 in Helsinki compared to 1716 in Berlin during 2016 [17]. Our analysis indicates that PV generation values in our dataset exceed standard residential ranges (7.5 kWh versus the typical 0.25–0.40 kWh per household [18]). To address this variance, we implemented a 0.1 calibration coefficient to maintain consistency with industry standards while retaining the integrity of temporal relationships.

2.2. Uncertainty Prediction

Comprehensive model formulations for both the SDDP and LP approaches can be found in Section 2, with a complete listing of terms and definitions available in the Nomenclature section.

Our forecasting approach integrates three key parameters into the analysis framework:

1. Day-ahead electricity spot market prices $\omega_{spr}^{spot} \in \Omega_{spr}^{spot}$ in EUR/kWh;
2. Residential electricity demand $\omega_{spr}^{dem} \in \Omega_{spr}^{dem}$ in kWh; and
3. Residential PV generation $\omega_{spr}^{pv} \in \Omega_{spr}^{pv}$ in kWh.

For day-ahead spot market electricity price forecasting, we employ a 20-stage exponential moving average methodology with a smoothing parameter (i.e., a tuning parameter) set to 2.0 to establish hourly price means ($\bar{X}$) [9,19]. The simple sample standard deviation is utilized to determine hourly price standard deviations (s). Subsequently, we generate three distinct hourly price scenarios from the Gaussian distribution based on the calculated hourly $\bar{X}$ and s values, representing the three uncertainty scenarios of spot market price uncertainties, ω_{spr}^{spot}. The second row of Figure 1 illustrates these three scenarios, denoted as s1–s3 (columns 1–3), alongside corresponding historical price data (column 4). The figure employs boxplot visualization to display hourly distribution ranges for data collected between 1 May 2023 and 1 August 2023.

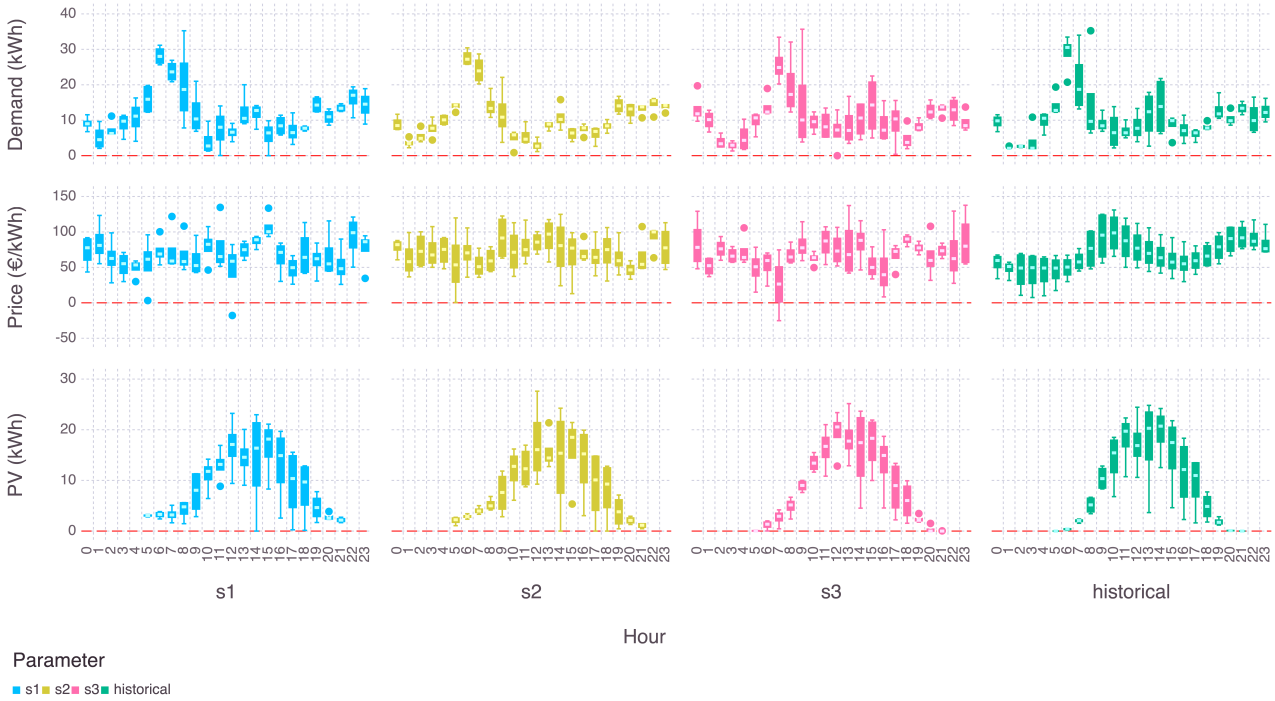

Figure 1. Input parameters of electricity consumption, electricity prices, and PV generation from 2 to 4 May 2023.

For PV generation and residential electricity consumption data, the analysis employs a three-scenario approach for each parameter, generating distinct predictions to account for varying conditions. Within each planning horizon $r \in R$, we utilize three prediction methodologies: exponential smoothing [9–11], seasonal auto-regressive integrated moving average (SARIMA) [7,11,12], and local-level cycle (LLC) [11,12]. These models are calibrated using historical data spanning 120 stages (i.e., hours) to forecast PV generation and electricity demand for the subsequent 12 stages (preliminary experiments have

shown that a 12-h horizon provides an optimal balance between prediction and computational performance. A detailed discussion concerning these experiments can be found in [20].) ($p = \{1, 2, \ldots, 12\}$). The resulting forecasts generate three distinct scenarios, $s = \{1, 2, 3\}$, for each uncertainty parameter (PV generation uncertainties, ω^{pv}_{spr}, and demand uncertainties, ω^{dem}_{spr}), which subsequently serve as input parameters for the SDDP model's optimization process. The first and third rows in Figure 1 present a visualization of three distinct scenarios, accompanied by historical data, pertaining to residential energy demand and amount of PV. The time-series analysis and uncertainty predictions were executed using the Julia package StateSpaceModels.jl [11].

Although uncertainty forecasting constitutes a significant component of our methodology, it serves primarily as an input generation mechanism for our SDDP model. The core objective of our research lies in the development and implementation of SDDP algorithms for battery operation optimization.

2.3. Linear Policy Graph Model Elements

We implement a multi-stage SDDP framework utilizing a linear policy graph approach. Figure 2 presents the architectural framework of our SDDP model. The following section outlines the essential terminology of our SDDP implementation [8,13]. This study incorporates four sets: stages ($p, q \in P$), planning horizons ($r \in R$), scenarios ($s \in S$), and uncertainties ($u \in U$).

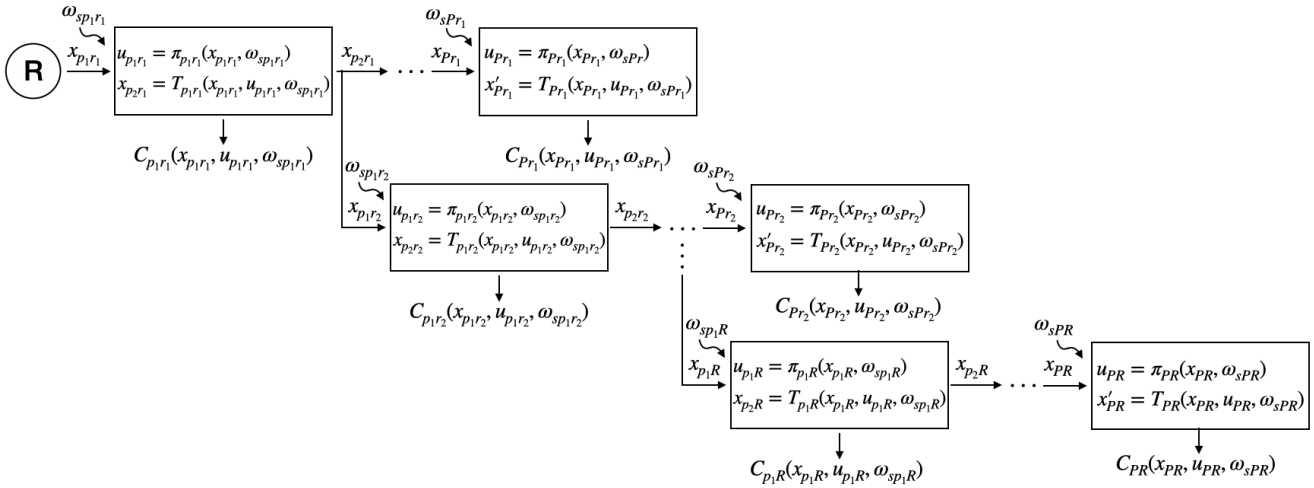

Figure 2. Linear policy graph in an SDDP model for each planning horizon $r \in R$.

Stage As shown in Figure 2, the linear policy graph comprises a structured set of nodes (depicted as rectangles) representing stages $p \in P$ (each one-hour long) and planning horizons $r \in R$ (arranged in rows). At each node, which marks a specific point in time, an agent (i.e., an SDDP model optimizer) selects an action based on the revealed uncertainty parameters ($\omega_{spr} \in \Omega_{spr}$).

Noise The model incorporates stochastic elements, represented as $\omega_{spr} \in \Omega_{spr}$, which maintain independence across sequential decision stages. These elements are characterized through a set of scenarios $s \in S$, each representing distinct probabilistic outcomes. The framework encompasses three primary categories of uncertainty parameters: $\omega^{spot}_{spr} \in \Omega^{spot}_{spr}$, $\omega^{dem}_{spr} \in \Omega^{dem}_{spr}$, and $\omega^{pv}_{spr} \in \Omega^{pv}_{spr}$.

State We represent the battery storage balance in kWh using the state variable x_{pr}. The decision-making sequence begins at the root node R (denoted by a circle) in Figure 2, where the initial battery storage balance $x_{p_1r_1}$ is established for the first stage (represented by the first square node in row one). The system then proceeds to determine

an outgoing state $x_{p_2r_1}$. The study's primary objective is to enhance battery storage efficiency through hourly operational optimization, taking into consideration three key variables: day-ahead spot market prices (ω_{spr}^{spot}), electricity demand (ω_{spr}^{dem}), and photovoltaic generation (ω_{spr}^{pv}). Within the hourly optimization framework, initial stage predictions ($p = 1 \in P$) demonstrate the highest accuracy in terms of uncertainty prediction compared to subsequent stages ($p = \{2, 3, \ldots, 12\} \in P$) across each planning horizon ($r = \{1, 2, \ldots, 72\} \in R$). As a result, decisions from the first stage of each planning horizon ($x_{p=2,r}$) systematically transition to the subsequent horizon's first stage ($x_{p=1,r+1}$), establishing a continuous connection between planning periods in a rolling-horizon manner, as depicted in Figure 2.

$u_{pr}(\cdot)$ The control variable ($u_{pr}|u_{pr} \in U_{pr}(x_{pr}, \omega_{spr})$) represents a decision made by an agent during a stage. We assume all control variables u_{pr} are discrete and feasible for an agent to implement. Our model incorporates four primary control variables: battery energy injection (b_{pr}^{inj}) and extraction (b_{pr}^{xtr}), alongside grid electricity purchase (e_{pr}^{pur}) and sales (e_{pr}^{sale}), measured in kWh.

$T_{pr}(\cdot)$ The transition function can take various forms [8], with each state transition resulting in an associated cost ($C_{pr}(\cdot)$), as shown in Figure 2.

$C_{pr}(\cdot)$ The stage cost function ($C_{pr}(x_{pr}, u_{pr}, \omega_{spr})$) represents the optimization objective that requires minimization at each stage pr. This cost function evaluates the financial impact of implementing control decisions u_{pr} on the state variable x_{pr}, taking into account the realization of uncertainty parameters ω_{spr}. In this study, the stage cost specifically refers to the household electricity bill.

$\pi_{pr}(\cdot)$ The decision rule, represented as π_{pr}, determines control variable u_{pr} through evaluation of the current state variable x_{pr} and observed uncertainties ω_{spr}. A set of these decision rules constitutes a policy ($\pi_{pr}\ \forall\ p \in P, r \in R$), where individual components align with specific stages p and planning horizons r.

Node Referring to Figure 2, our multistage SDDP framework is structured around interconnected nodes. Each node incorporates key operational elements: state variables x_{pr}, noise ω_{spr}, control variables u_{pr}, transition function T_{pr}, stage objective C_{pr}, and decision rules π_{pr}. To demonstrate the policy graph structure, we implement a hazard-decision node framework, wherein operational decisions u_{pr} are executed at each stage following the realization of noise $\omega_{spr} \in \Omega_{spr}$.

2.4. Model Assumptions

The model incorporates the following key operational parameters and assumptions:

1. The battery storage system operates with an hourly energy injection and extraction rate (C^{rate}) of 25% capacity, based on specifications of a Lithium-ion battery (LFP) rated at 2 kW for 4 h. The maximum charging (b_{pr}^{inj}) and discharging (b_{pr}^{xtr}) limits are set by C^{rate} times maximum capacity ($\overline{B}^{bal}$). The system maintains injection and extraction efficiencies (E^{inj} and E^{xtr}) of ($\sqrt{83}$)%, yielding an 83% round-trip efficiency [21].
2. Battery self-discharge effects were deemed negligible over the 72 h modeling period, allowing for the simplification of E^{bal} to remain at a constant value of 1.
3. To ensure operational reliability, a minimum battery storage level ($\underline{B}^{bal}$) of 20% capacity is maintained as a strategic power reserve.
4. The system is initialized with a battery charge level (B^{init}) of 20% capacity.
5. The model incorporates a design to address end-of-horizon effects through the implementation of SDDP and LP models. Within the rolling-horizon framework, each horizon spans 12 stages. The battery balance b_{pr}^{bal}, functioning as a state variable, is strategically transferred from the second stage of the current horizon to serve as an

initial input for the first stage of the subsequent horizon. This ensures operational continuity by transferring the battery storage balance between consecutive planning horizons ($r+1|r=\{1,\ldots,R-1\}$), as detailed in Section 2.5 and Figure 2.

6. While extreme market conditions like price volatility and power outages are acknowledged, they fall outside the scope of this analysis to maintain methodological focus.
7. The optimization scope is specifically limited to battery charging and discharging strategies, excluding considerations of PV system optimization through solar tracking mechanisms or panel orientation adjustments.

The successful implementation of stochastic dual dynamic programming relies on adherence to fundamental assumptions, as outlined in [8,14,20]. To implement and solve Equation (1), we employ SDDP.jl, a Julia package developed in [14].

2.5. Sub-Problems of the SDDP Model

$$\min \quad \mathbb{S} = \sum_{r\in R}\sum_{p\in P}\Bigg[\Big((1+V)\sum_{s\in S}\mathbb{P}_{spr}\omega^{spot}_{spr}+C^{pur}\Big)e^{pur}_{pr}+C^{batt}(b^{inj}_{pr}+b^{xtr}_{pr}) \tag{1a}$$

$$+C^{pv}\sum_{s\in S}(\mathbb{P}_{spr}\omega^{pv}_{spr})-\Big(\sum_{s\in S}\mathbb{P}_{spr}\omega^{spot}_{spr}-C^{sale}\Big)e^{sale}_{pr}\Bigg]$$

$$s.t. \quad e^{sale}_{pr}+b^{inj}_{pr}+\sum_{s\in S}(\mathbb{P}_{spr}\omega^{dem}_{spr})=e^{pur}_{pr}+b^{xtr}_{pr}+\sum_{s\in S}(\mathbb{P}_{spr}\omega^{pv}_{spr}) \quad \forall\, p\in P,\ r\in R \tag{1b}$$

$$E^{bal}b^{bal}_{pr}+E^{inj}b^{inj}_{pr}-E^{xtr}b^{xtr}_{pr}=E^{bal}b^{bal}_{(p+1)r}\ \forall\, p=1,\ldots,P-1,\ r\in R \tag{1c}$$

$$\overline{B}^{bal}\geq b^{bal}_{pr} \quad \forall\, p\in P,\ r\in R \tag{1d}$$

$$b^{bal}_{pr}\geq \underline{B}^{bal} \quad \forall\, p\in P,\ r\in R \tag{1e}$$

$$b^{bal}_{(p=1)(r=1)}=B^{init},\ p=1|p\in P, r=1|r\in R \tag{1f}$$

$$b^{bal}_{p=1,r+1}=b^{bal}_{p=2,r},\ p=\{1,2\}|p\in P,\ r=\{1,\ldots,R-1\}\in R \tag{1g}$$

$$C^{rate}\overline{B}^{bal}\geq b^{inj}_{pr} \quad \forall\, p\in P,\ r\in R \tag{1h}$$

$$C^{rate}\overline{B}^{bal}\geq b^{xtr}_{pr} \quad \forall\, p\in P,\ r\in R \tag{1i}$$

$$b^{bal}_{pr}, b^{inj}_{pr}, b^{xtr}_{pr}, e^{pur}_{pr}, e^{sale}_{pr}\geq 0 \tag{1j}$$

Our mathematical formulation leverages and extends established methodologies from prior research [20,22–24], integrating energy conservation principles for battery storage systems with real-world physical and economic limitations.

The SDDP framework incorporates sub-problems formulated as multi-stage linear programming models, as detailed in Equation (1). The objective function in Equation (1a) aims to optimize financial performance by minimizing total expected costs while accounting for revenue across all planning horizons $r\in R$, stages $p\in P$, and scenarios $s\in S$. The SDDP approach has $\mathbb{P}_{spr}=1/3$ with the constraint that scenario probabilities sum to unity ($\sum_s^S \mathbb{P}_{spr}=1.0\ \forall\, p\in P,\ r\in R$). The equal probability of $1/3$ is assigned to each prediction as the three forecasting models demonstrate comparable levels of accuracy in their predictive capabilities (model performance comparisons from the previous work [20] revealed no significant differences in MAE, MSE, and RMSE metrics among these three models when compared to historical data. The prediction results (which become scenarios 1–3) are shown in Figure 1.). Equation (1a) encompasses three cost components and one revenue stream. The first cost component calculates the total expense of grid-purchased electricity. This is determined by multiplying the purchased electricity volume (e^{pur}_{pr}) by the projected spot-market rate (ω^{spot}_{spr}) for each scenario $s\in S$, weighted by their respective probabilities $\mathbb{P}_{spr}$. This is then adjusted with purchasing taxes V in EUR/kWh. Finally,

the expected taxed spot-market cost is added to the network's marginal purchasing fees C^{pur} in EUR/kWh. Note that taxation is applicable exclusively to electricity purchases [25]. Battery-related operational costs are incurred on the energy flows into and out of the storage system (b^{inj}_{pr} and b^{xtr}_{pr}), with each flow being assessed at the standard battery utilization cost of C^{batt} in EUR/kWh. The third cost component reflects the anticipated photovoltaic (PV) generation, calculated by aggregating the expected generation (ω^{pv}_{spr}) across all scenarios, weighted by their respective probability factors ($\mathbb{P}_{spr}$), and multiplied by the associated unit cost (C^{pv}) expressed in EUR/kWh. Sale revenue is derived from selling surplus energy back to the grid. The compensation rate is determined by multiplying the sold energy volume (e^{sale}_{pr}) in kWh by the unit price in EUR per kWh. This unit price incorporates the weighted average spot-market rate (ω^{spot}_{spr}) across scenarios $s \in S$ based on their probabilities $\mathbb{P}_{spr}$, adjusted for network sale fees (C^{sale}) in EUR/kWh.

Equation (1b) establishes energy balance requirements across all stages ($p \in P$) and planning horizons ($r \in R$). On the demand side, this encompasses energy sold e^{sale}_{pr}, energy injected b^{inj}_{pr}, and probability-weighted demand ω^{dem}_{spr} representing average households' demand. The supply components comprise purchased energy e^{pur}_{pr}, extracted energy b^{xtr}_{pr}, and probability-weighted PV generation ω^{pv}_{spr}. Equation (1c) calculates the battery's energy storage level for the next stage $b^{bal}_{(p+1)r}$ by considering three key elements: the present stored energy b^{bal}_{pr}, energy injection b^{inj}_{pr}, and energy extraction b^{xtr}_{pr}. The corresponding efficiency coefficients E^{bal}, E^{inj}, and E^{xtr} are incorporated as specified in Section 2.4. Equation (1d,e) establish the operational limits for battery capacity. Specifically, Equation (1e) maintains a minimum charge level to prevent complete battery depletion during optimization. The initial balance of the battery storage for the first stage and the first planning horizon ($b^{bal}_{(p=1)(r=1)}$) is determined by Equation (1f). The model optimizes hourly schedules across multiple planning horizons ($r \in R$), with each horizon comprising multiple stages ($p \in P$). The battery storage balance (b^{bal}_{pr}) serves as the only state variable, facilitating continuity between planning horizons through a rolling-horizon approach. As specified in Equation (1g), the battery storage level transitions from the second stage of the current planning horizon ($b^{bal}_{(p=2)r}$) to the first stage of the subsequent horizon ($b^{bal}_{(p=1)(r+1)}$). Equation (1h,i) establish operational constraints for the battery storage system by defining maximum thresholds for energy injection (b^{inj}_{pr}) and extraction (b^{inj}_{pr}) amounts. All variables are non-negative, as outlined in Equation (1j).

2.6. Algorithms

It is important to state the inherent differences between linear programming (LP) and stochastic dual dynamic programming (SDDP) models. The LP model operates with complete future information (i.e., perfect foresight), whereas the SDDP model manages real-world uncertainties in electricity prices, demand, and PV generation through probabilistic scenarios. As such, we utilize the LP model as a theoretical upper bound for system performance, while the SDDP model provides practical, implementable solutions under uncertainty. The relative performance of these approaches varies based on the accuracy of forecasted parameters and the magnitude of uncertainties in the system. The detailed implementation procedures for SDDP and LP approaches are presented in Algorithms 1 and 2, respectively.

2.6.1. The SDDP Model

During Step 2, the model utilizes historical data (120 prior hours) for each period p, r to forecast three uncertainty parameters (ω^{spot}_{spr}, ω^{dem}_{spr}, and ω^{pv}_{spr}), generating $\Omega^{predict}_{spr}$, as described in Section 2.2. The trained SDDP model, $\mathbb{M}^{SDDP}$, is implemented in Step 3, utilizing the predicted uncertainty set, $\Omega^{\text{predict}}_{\text{spr}}$, established in the preceding step. In Step 4,

the model incorporates historical uncertainty values (120 prior hours), designated as Ω_{spr}^{real}. Ω_{spr}^{real} represents the empirical dataset comprising residential demand patterns, electricity pricing data, and PV generation measurements in kWh for the period spanning 1 May 2023 through 1 August 2023, as illustrated in the fourth column of Figure 1. $\Omega_{\text{spr}}^{\text{predict}}$ in Step 2 serves as the training dataset for the SDDP model ($\mathbb{M}^{SDDP}$), whereas Ω_{spr}^{real} in Step 4 is utilized to evaluate associated costs in Equation (1a) using the trained SDDP model. Subsequently, these values (Ω_{spr}^{real}) are used in the computation of stage-specific objectives in Step 5, specifically determining the associated costs for each period and planning horizon ($p \in P, r \in R$). The variable $C_{(p=1)r}$ denotes the first-stage cost, while $\mathbb{C}_{(p=2,\ldots,12)r}^{cost-to-go}$ encompasses the cost-to-go from the second to the twelfth period for each planning horizon $r \in R$. The aggregate costs from stage p to $p+11$ comprise the stage objective at the current stage, determined by the implemented control u and policy π, combined with the cost-to-go function spanning stages $p+1$ through $p+11$ [8]. The aggregation of costs across all periods (combining $C_{(p=1)r}$ with $\mathbb{C}_{(p=2,\ldots,12)r}^{cost-to-go}$) is performed and aggregated across planning horizons $r \in R$ in Step 6, yielding the final SDDP solution, $\mathbb{S}^{SDDP}$, in the final step.

Algorithm 1 SDDP

1: SDDP(*case*)
2: $\Omega_{spr}^{predict} \leftarrow$ Predict uncertainties
3: $\mathbb{M}^{SDDP} \leftarrow$ Solve Equation (1) using $\Omega_{spr}^{predict}$
4: $\Omega_{spr}^{real} \leftarrow$ Assign uncertainties with historical values
5: $C_{(p=1)r}, \mathbb{C}_{(p=2,\ldots,12)r}^{cost-to-go} \leftarrow$ Evaluate $\mathbb{M}^{SDDP}$ with Ω_{spr}^{real}
6: $\mathbb{S}^{SDDP} \leftarrow \sum_{r \in R}(C_{(p=1)r} + \mathbb{C}_{(p=2,\ldots,12)r}^{cost-to-go})$
7: **return** $\mathbb{S}^{SDDP}$

2.6.2. The LP Model

In contrast to the SDDP approach, the LP model incorporates historical data (Ω_{spr}^{real}) at Step 2 and operates with a single scenario ($s = \{1\} | s \in S$) in Equation (1), whereas SDDP utilizes three scenarios ($s = \{1,2,3\} | s \in S$). This applies to ω_{spr}^{dem}, ω_{spr}^{pv}, and ω_{spr}^{spot}, which implies that the LP model has access to perfect information. The model then proceeds to compute $\mathbb{S}^{LP}$ (i.e., the solution of the LP model) across all periods $p \in P$ and planning horizons $r \in R$ in Step 3, with the final value being output in the concluding step.

Algorithm 2 LP

1: LP(*case*)
2: $\Omega_{spr}^{real} \leftarrow$ Assign uncertainties with historical values
3: $\mathbb{S}^{LP} \leftarrow$ Solve Equation (1) using Ω_{spr}^{real}
4: **return** $\mathbb{S}^{LP}$

3. Case Study

This study examines battery storage optimization approaches through a comprehensive analysis of three SDDP model variants, utilizing an LP model as an idealized benchmark. To assess storage capacity effects, we analyze various battery configurations from 0 to 2000 kWh in 500 kWh intervals. Section 2 provides an in-depth comparison of these methodological frameworks. The investigation was conducted from 2 to 5 May 2023, as shown in Figure 3 (The model labels in Figures 3–5 use a consistent naming convention: case number, case designation, model methodology, and battery capacity. For instance,

"C1_BASE_SDDP_0" indicates Case 1 (baseline scenario) using the SDDP model with 0 kWh battery storage capacity.).

Figure 3. Battery storage balance in kWh.

The cost parameters implemented in Equation (1) are derived from established industry sources [25,26], ensuring the model reflects current market conditions. The electricity purchase and sale marginal costs (C^{pur}, C^{sale}) are set at 0.0421 EUR/kWh and 0.00211 EUR/kWh respectively [25]. The operational costs include 0.006 EUR/kWh for PV generation (C^{PV}) [27,28] and 0.002 EUR/kWh for battery storage utilization (C^{batt}) [4,21]. A value-added tax (VAT) rate (V) of 20% is applied to these values.

The analysis encompasses four distinct case studies, each featuring specific configurations of electricity pricing and photovoltaic (PV) generation parameters. The following cases have been established for evaluation:

1. C1_BASE_SDDP: The baseline scenario serves as our control case, incorporating baseline operational parameters for demand, PV generation, and spot market pricing as illustrated in Figure 1 [25,26].
2. C2_HEP_SDDP: The high electricity pricing (HEP) scenario examines system performance by implementing a twofold increase in electricity costs compared to the baseline parameters.
3. C3_HPV_SDDP: The high PV generation (HPV) scenario assesses system operation under conditions where photovoltaic output is doubled relative to baseline measurements.
4. C4_BASE_LP: A comparative analysis utilizing linear programming methodology while maintaining baseline parameters.

3.1. Comparing Performance Metrics Between SDDP and LP Models

Our analysis examines the performance metrics between two models: the SDDP model (C1_BASE_SDDP) and the LP model (C4_BASE_LP). This analysis evaluates the financial implications for residents through examination of objective function values as defined in

Equation (1a), which quantifies energy costs. The LP model calculates objective function values by aggregating financial savings across 12-hourly stages within each planning horizon. The SDDP model, on the other hand, evaluates financial savings by integrating the initial stage objective function value with expected cost-to-go function values throughout the final stage, as detailed in Section 2.

Table 1 presents a quantitative assessment of performance metrics that contrasts SDDP and LP models at varying battery storage capacities. The analysis incorporates statistical measures of objective function values for both modeling approaches, supported by statistical hypothesis testing to evaluate the equivalence of means between SDDP and LP implementations at corresponding battery storage capacities. In our statistical analysis, we designate the SDDP model and LP model as X and Y, respectively. The sample means of the objective function values are denoted as $\overline{X}$ for SDDP and $\overline{Y}$ for LP, with n representing the sample size. The population means are represented by μ_X for SDDP and μ_Y for LP, while the standard deviations are denoted as s_X and s_Y for their respective models. Given that both $\overline{X}$ and $\overline{Y}$ consist of large independent samples, they are approximately normally distributed [20]. The null distribution of $\overline{X}$ - $\overline{Y}$ can be stated as $\overline{X}$ - $\overline{Y} \sim N(\mu_x - \mu_y, \sigma^2_{\overline{X}} + \sigma^2_{\overline{Y}}) = N(\mu_x - \mu_y, \sigma^2_X/n_X + \sigma^2_Y/n_Y)$ [29]. We used sample variances s^2_X and s^2_Y to estimate the unknown population variances σ^2_X and σ^2_Y. The null and alternate hypotheses are $H_0 : \mu_X - \mu_Y = 0$ versus $H_1 : \mu_X - \mu_Y \neq 0$. The statistical significance of the differences between models is evaluated using p-values shown in Table 1. These values are derived from a two-tailed test calculation where $p(x \leq -|z| \text{ or } x \geq |z|)$, with the z-score determined using the formula $z = ((\overline{X} - \overline{Y}) - \Delta_0)/(\sqrt{s^2_X/n_X + s^2_Y/n_Y})$ and Δ_0 set to 0.

Table 1. Comparison of objective function values between SDDP (X) and LP (Y) models.

	0 kWh		500 kWh		1000 kWh		1500 kWh		2000 kWh	
	X	Y	X	Y	X	Y	X	Y	X	Y
n	72	72	72	72	72	72	72	72	72	72
min	−101.158	−7.884	−106.021	−71.612	−112.144	−134.89	−118.267	−198.168	−119.642	−263.263
average	−10.119	5.377	−38.064	−32.436	−63.577	−69.610	−64.058	−106.783	−64.247	−143.956
max	15.955	15.220	1.846	6.749	−10.156	4.341	−5.058	1.933	−5.963	−0.474
s	37.645	5.599	29.936	17.844	28.558	33.229	28.988	48.868	29.298	64.576
$\Delta = (\overline{Y} - \overline{X}) \cdot 100/\overline{X}$	−153.14%		−14.79%		9.49%		66.70%		124.07%	
p-value	0.0006		0.1706		0.2427		0.0000		0.0000	

For our statistical analysis, we employ a significance level of $\alpha = 0.05$ as our threshold for hypothesis testing. When p-value falls below α, we reject H_0, showing substantial evidence against the statistical equivalence between SDDP and LP model means at the 95% confidence level. This occurred at battery storage capacities of 0, 1500, and 2000 kWh. Conversely, for storage capacities of 500 and 1000 kWh, analysis revealed p-values above the α threshold. These results suggest insufficient statistical evidence to establish significant performance variations between the models at the 95% confidence level. Although the LP model's perfect foresight suggests it should produce optimal solutions (means in Table 1) compared to the SDDP model, the observed performance variance stems from their differentiated data-processing methodologies. The LP model processes historical hourly data, whereas the SDDP model employs equal probability distributions across three scenarios per hour (detailed in Section 2). Given that predictions can encompass a broader range of values compared to historical data, this methodological difference results in LP potentially yielding worse average objective function values than SDDP (where lower values indicate better performance). This discrepancy is evident in the average objective function values when comparing SDDP and LP implementations with 0 kWh and 500 kWh battery storage capacities, as demonstrated in Table 1. Despite the SDDP model's initial advantage due to its broader input data range, the LP model demonstrates superior performance with battery capacities ranging from 1000 kWh to 2000 kWh. This

indicates that battery storage systems effectively function as a temporal shifting mechanism, enabling residents to optimize their financial savings.

3.2. Evaluating Market Dynamics: Electricity Price Volatility and Photovoltaic Generation Variability

Our analysis evaluates the performance differences between scenarios with high electricity prices (C2_HEP_SDDP) and high PV generation (C3_HPV_SDDP), comparing these against baseline configurations (C1_BASE_SDDP and C4_BASE_LP). Each scenario incorporates distinct battery storage capacities, as outlined in Section 3.

The analysis reveals notable diurnal patterns in battery utilization in kWh, characterized by enhanced charging activities during daylight hours (i.e., 05:00 to 21:00) in correlation with PV generation, followed by increased discharge operations during peak demand periods in Figure 3. Furthermore, the data indicates more measured fluctuations in battery usage within SDDP models when compared to the LP methodology. The C2_HEP_SDDP model exhibits conservative battery utilization patterns, which can be attributed to elevated electricity prices, with battery capacity showing limited influence on battery utilization. The analysis of C3_HPV_SDDP reveals unvarying operational patterns, indicating efficient utilization of photovoltaic generation resources. In contrast, C4_BASE_LP demonstrates more intensive charging and discharging behavior, particularly evident in scenarios with increased battery capacity. The comparison between C1_BASE_SDDP and C4_BASE_LP reveals distinct operational strategies in their battery utilization and capacity management protocols. While C4_BASE_LP exhibits a direct relationship between battery size and utilization, C1_BASE_SDDP demonstrates a more sophisticated approach. This distinction arises from SDDP's implementation of 12 h forecasting across three scenarios to optimize battery storage allocation. By incorporating variables such as PV generation uncertainty, energy consumption patterns, and electricity price fluctuations, the SDDP framework adopts a more measured approach to battery utilization compared to LP's deterministic methodology.

Figure 4 presents our analysis of two fundamental metrics: energy purchases, displayed in the upper portion of each bar graph in blue, and energy sales, shown in the lower portion in yellow. Both metrics are measured in kilowatt-hours (kWh). This visualization compares energy trading patterns across different model configurations on the x-axis, focusing on the total volume of energy exchanges in kWh. Generally, peak trading activities are observed in model C4_BASE_LP that exhibit significantly higher trading volumes due to taking advantage of its perfect information about uncertainties. By comparison, the three SDDP model variants (C1_BASE_SDDP, C2_HEP_SDDP, C3_HPV_SDDP) demonstrate more conservative and strategic trading patterns. The C2_HEP_SDDP configuration demonstrates reduced trading volumes compared to C1_BASE_SDDP, primarily due to elevated electricity prices, which leads to decreased purchasing activity to mitigate price volatility and manage battery storage charging. The C3_HPV_SDDP configuration exhibits the most modest trading volumes across all four categories, attributed to its substantial photovoltaic generation capacity, which diminishes the requirement for external electricity purchases. The comparative analysis indicates that C4_BASE_LP model iterations demonstrate notably increased trading volumes in comparison to the three SDDP model variants, which highlights potential opportunities for enhancing SDDP's optimization capabilities and trading strategy implementation.

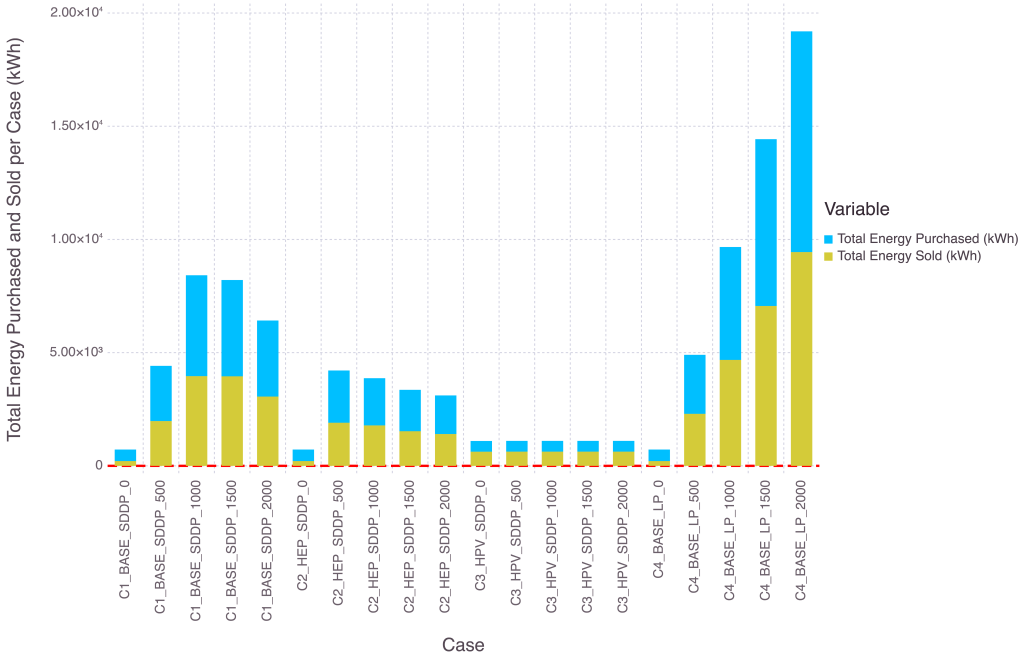

Figure 4. Analysis of grid energy exchange: evaluating electricity purchase and sale patterns across case studies and battery storage capacities.

The results show financial savings measured in euros (€) for each contiguous 12 h period (i.e., a planning horizon) during 2–5 May 2023, as depicted in Figure 5. The box plot analysis reveals distinct financial saving distributions across the case studies. Negative values in the box-plots indicate revenue from selling electricity back to the grid. This occurs when photovoltaic generation exceeds residential consumption, mainly during daytime hours when residents are at work. The data demonstrates notable variance in outcomes, with C4_BASE_LP exhibiting particularly pronounced variability. There are statistical outliers at both extremes of the distribution, as seen in the dots. Examination of median trends reveals a systematic improvement in savings efficiency (with lower values indicating better performance) as battery capacity increases across case studies. The sensitivity analysis demonstrates that the relationship between battery capacity and financial performance is not strictly linear. In scenarios C1_Base_SDDP and C2_HEP_SDDP, we observe that battery capacities beyond 1000 kW and 500 kW respectively yield minimal additional revenue benefits, as evidenced by the statistical insignificance in median values beyond these thresholds. This limitation is primarily attributed to constraints in available PV generation capacity. In contrast, scenario C3_HPV_SDDP shows linear performance improvements with increased battery capacity due to abundant PV generation. This scenario achieves better savings through higher PV generation, while using minimal battery storage and grid trading (see Figures 3 and 4). The C4_BASE_LP configuration exhibits enhanced operational efficiency through its perfect foresight, facilitating enabling battery storage management relative to alternative scenarios. These results establish an idealized benchmark for evaluating system optimization capabilities.

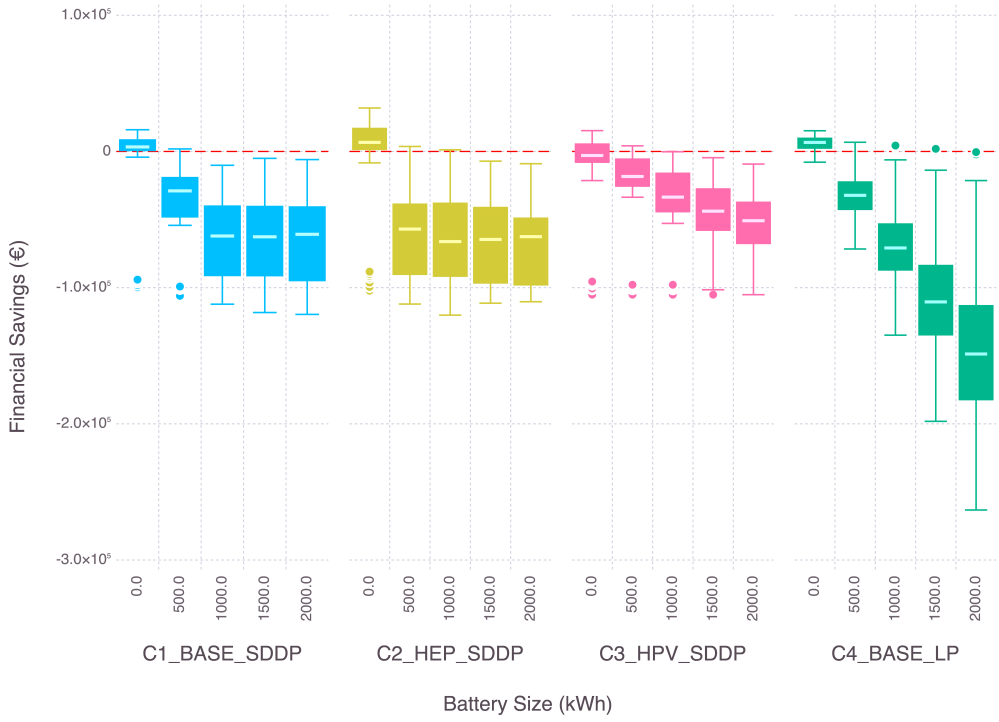

Figure 5. Financial savings analysis (EUR) across case study scenarios, where positive values indicate costs and negative values represent revenues from selling electricity back to the grid.

4. Conclusions

This research presents a methodology for optimizing residential battery storage through strategic energy management. Our approach combines a linear policy graph [8] with the stochastic dual dynamic programming (SDDP) algorithm [6] to create robust energy management solutions for communities using battery storage systems. Through strategic optimization of battery charging and discharging cycles, we achieve substantial cost reductions. The SDDP optimization framework effectively manages battery operations across variable pricing scenarios while maintaining computational efficiency. To evaluate our approach, we incorporate linear programming (LP) methodology as an idealized benchmark. Our analysis shows that the SDDP model achieves comparable performance metrics to its LP counterpart. The results demonstrate both the economic feasibility for residential communities and the environmental benefits of integrated PV and battery storage systems, particularly in reducing energy bills. Our assessment validates the energy management capabilities of SDDP models. While the LP implementation shows direct proportionality between battery capacity and optimization potential, SDDP scenarios reveal more nuanced relationships due to operating under uncertainty—incorporating variations in generation, demand, and pricing parameters.

Our analysis demonstrates that the model delivers substantial environmental advantages through its advanced energy management capabilities. The system achieves environmental benefits through two key mechanisms: optimal energy storage scheduling aligned with renewable energy availability, and strategic load-shifting during periods of high energy demand. Although environmental impact was not our primary research focus, the integration of PV generation with battery storage systems has yielded measurable reductions in emissions and reliance on conventional fossil-fuel-based power generation methods [20,24].

The model has been developed and preliminarily validated through simulations for battery storage system implementation. Full-scale physical testing remains beyond our current scope but is recommended for future research to validate real-world applications.

Author Contributions: Conceptualization, P.C., F.O. and S.A.G.; methodology, P.C., F.O. and S.A.G.; software, P.C.; validation, P.C. and F.O.; formal analysis, P.C., F.O. and S.A.G.; investigation, P.C.; resources, F.O.; data curation, P.C. and F.O.; writing—original draft preparation, P.C.; writing—review and editing, P.C., F.O. and S.A.G.; visualization, P.C.; supervision, F.O. and S.A.G.; project administration, F.O.; funding acquisition, F.O. All authors have read and agreed to the published version of the manuscript.

Funding: The work in this project was funded by the Academy of Finland under Application No. 348094.

Data Availability Statement: The data presented in this study are available on request from the corresponding author.

Conflicts of Interest: The authors declare no conflicts of interest.

Abbreviations

The following abbreviations are used in this manuscript:

ARIMA	auto-regressive integrated moving average
LP	linear programming
SDDP	stochastic dual dynamic programming
VRE	variable renewable energy

Nomenclature

The general terminology for stochastic dual dynamic programming (SDDP) is outlined below. Multistage refers to a series of decisions made by an agent (such as an optimizer) over time to achieve optimal results. Stochastic pertains to scenarios where decisions need to be made under uncertainty, unfolding sequentially over multiple stages. A node serves as a decision point for an agent, featuring two primary types of variables in the research: state variables and control variables. State variables monitor system attributes over time, whereas control variables represent actions by the agent within a node that influence state variables.

Indices, Sets, Symbols

$p, q \in P$	Index and set of node or predicted stages
$r \in R$	Index and set of planning horizon
$s \in S$	Index and set of scenarios
$u \in U$	Index and set of types of uncertainties, $u = \{price,\ demand,\ PV\}$

Parameters

$\underline{B}^{bal}$	Minimum capacity of a battery storage (kW) $\forall\ p \in P,\ r \in R$
B^{init}	Initial balance of the battery storage (kWh)
$\overline{B}^{bal}$	Maximum capacity of a battery storage (kW) $\forall\ p \in P,\ r \in R$
C^{batt}	Battery storage utilization cost (EUR/kWh)
C^{PV}	PV generation cost (EUR/kWh)
C^{pur}	Marginal cost for residents to purchase electricity in stage $p \in P$ (EUR/kWh)
C^{rate}	A battery's charge and discharge rates (%)
C^{sale}	Marginal cost for residents to sell electricity in stage $p \in P$ (EUR/kWh)
E^{bal}	Availability factor of hourly battery storage holding efficiency (%)
E^{inj}	Availability factor of battery storage injection efficiency (%)
E^{xtr}	Availability factor of battery storage extraction efficiency (%)
$\mathbb{P}_{spr}$	Probability of occurrence for each stage $p \in P$ and scenario $s \in S$ (%),

given $\sum_s \mathbb{P}_{sp} = 1, \ \forall\ p \in P$

ω_{spr} An observed values of uncertainties

V Taxes to be added for purchasing electricity from the spot market (%)

Variables

b_{pr}^{bal} An amount of battery balance, a state variable, at the end of stage $p \in P$ for planning horizon $r \in R$ (kWh)

b_{pr}^{inj} An amount of battery injection, a control variable, at the start of stage $p \in P$ for planning horizon $r \in R$ (kWh)

b_{pr}^{xtr} An amount of battery extraction, a control variable, at the start of stage $p \in P$ for planning horizon $r \in R$ (kWh)

e_{pr}^{pur} Amount of purchased electricity, a control variable, $\forall\ p \in P,\ r \in R$ (kWh)

e_{pr}^{sale} Amount of electricity sold, a control variable, $\forall\ p \in P,\ r \in R$ (kWh)

References

1. Huttunen, R.; Kinnunen, M.; Lemström, B.; Hirvonen, P.; Kuuva, P. *Finland's Integrated National Energy and Climate Plan: Update*; Ministry of Economic Affairs and Employment of Finland: Helsinki, Finland, 2024.
2. VTT. *Project Details: Enabling Demand Response Through Easy to Use Open Source Approach*; Academy of Finland Project; Finnish Technical Research Centre (VTT): Espoo, Finland, 2021. Available online: https://cris.vtt.fi/en/projects/enabling-demand-response-through-easy-to-use-open-source-approach (accessed on 21 May 2023).
3. Denholm, P.; Nunemaker, J.; Gagnon, P.; Cole, W. The potential for battery energy storage to provide peaking capacity in the United States. *Renew. Energy* **2020**, *151*, 1269–1277. [CrossRef]
4. Mongird, K.; Fotedar, V.; Viswanathan, V.; Koritarov, V.; Balducci, P.; Hadjerioua, B.; Alam, J. HydroWIRES, Pacific Northwest National Laboratory (PNNL): Energy Storage Technology and Cost Characterization Report. 2019. Available online: https://energystorage.pnnl.gov/pdf/pnnl-28866.pdf (accessed on 21 May 2023).
5. Liu, D.; Xu, Y.; Wei, Q.; Liu, X. Residential energy scheduling for variable weather solar energy based on adaptive dynamic programming. *IEEE/CAA J. Autom. Sin.* **2018**, *5*, 36–46. [CrossRef]
6. Pereira, M.V.F.; Pinto, L.M.V.G. Multi-stage stochastic optimization applied to energy planning. *Math. Program.* **1991**, *52*, 359–375. [CrossRef]
7. Conejo, A.J.; Carrión, M.; Morales, J.M. *Decision Making Under Uncertainty in Electricity Markets*; Springer: New York, NY, USA, 2010. [CrossRef]
8. Dowson, O. The policy graph decomposition of multistage stochastic programming problems. *Networks* **2020**, *76*, 3–23. [CrossRef]
9. Hyndman, R.J. *Forecasting with Exponential Smoothing: The State Space Approach*; Springer series in statistics; Springer: Berlin/Heidelberg, Germany, 2008.
10. Hyndman, R.J.; Athanasopoulos, G. *Forecasting: Principles and Practice*, 2nd ed.; Otexts, Online, Open-Access Textbook: Lexington, KY, USA, 2018.
11. Saavedra, R.; Bodin, G.; Souto, M. StateSpaceModels.jl: A Julia package for time-series analysis in a state-space framework. *arXiv* **2019**, arXiv:1908.01757.
12. Durbin, J.; Koopman, S.J. *Time Series Analysis by State Space Methods*, 2nd ed.; Oxford University Press: Oxford, UK, 2012. [CrossRef]
13. Downward, A.; Dowson, O.; Baucke, R. Stochastic dual dynamic programming with stagewise-dependent objective uncertainty. *Oper. Res. Lett.* **2020**, *48*, 33–39. [CrossRef]
14. Dowson, O.; Kapelevich, L. SDDP.jl: A Julia package for stochastic dual dynamic programming. *INFORMS J. Comput.* **2021**, *33*, 27–33. [CrossRef]
15. CoSSMic. Detailed Household Load and Solar Generation in Minutely to Hourly Resolution, Collaborating Smart Solar-Powered Microgrids (CoSSMic). 2020. Available online: https://data.open-power-system-data.org/household_data/ (accessed on 21 May 2023).
16. ENTSO-E. ENTSO-E Transparency Platform: Day-Ahead Prices. Available online: https://transparency.entsoe.eu/dashboard/show (accessed on 16 February 2025).
17. PVGIS. Photovoltaic Geographical Information System (PVGIS), the European Commission's Joint Research Center. 2016. Available online: https://re.jrc.ec.europa.eu/pvg_tools/en/ (accessed on 3 March 2025).
18. Allen, N. How Much Power Does a Solar Panel Produce? 2022. Available online: https://www.forbes.com/home-improvement/solar/how-much-power-does-a-solar-panel-produce/ (accessed on 1 August 2024).

19. Chen, J. What Is EMA? How to Use Exponential Moving Average with Formula. 2024. Available online: https://www.investopedia.com/terms/e/ema.asp (accessed on 3 March 2025).
20. Chanpiwat, P. Three Essays on Optimization, Machine Learning, and Game Theory in Energy. Ph.D. Thesis, University of Maryland, College Park, MD, USA, 2023.
21. PNNL. *Lithium-Ion Battery (LFP and NMC), Energy Storage Cost and Performance Database*; Pacific Northwest National Laboratory (PNNL): Richland, WA, USA, 2025. Available online: https://www.pnnl.gov/projects/esgc-cost-performance/lithium-ion-battery (accessed on 3 March 2025).
22. Gabriel, S.A.; Conejo, A.J.; Fuller, J.D.; Hobbs, B.F.; Ruiz, C. *Complementarity Modeling in Energy Markets*; Springer: New York, NY, USA, 2012; p. 655.
23. Virasjoki, V.; Rocha, P.; Siddiqui, A.S.; Salo, A. Market impacts of energy storage in a transmission-constrained power system. *IEEE Trans. Power Syst.* **2016**, *31*, 4108–4117. [CrossRef]
24. Chanpiwat, P.; Gabriel, S.A.; Brown, M. Multi-stage modeling with recourse decisions for solving stochastic complementarity problems with an application in energy. *IEEE Trans. Power Syst.* **2024**, *39*, 4935–4948. [CrossRef]
25. Puranen, P.; Kosonen, A.; Ahola, J. Techno-economic viability of energy storage concepts combined with a residential solar photovoltaic system: A case study from Finland. *Appl. Energy* **2021**, *298*, 117199. [CrossRef]
26. Wehrmann, B. What German Households Pay for Electricity. 2015. Available online: https://www.cleanenergywire.org/factsheets/what-german-households-pay-electricity (accessed on 17 May 2023).
27. IEA. *Renewables 2023: Analysis and Forecast to 2028*; International Energy Agency (IEA): Paris, France, 2023. Available online: https://iea.blob.core.windows.net/assets/96d66a8b-d502-476b-ba94-54ffda84cf72/Renewables_2023.pdf (accessed on 7 March 2024).
28. IRENA. *Renewable Power Generation Costs in 2023*; International Renewable Energy Agency (IRENA): Abu Dhabi, United Arab Emirates, 2024. Available online: https://www.irena.org/-/media/Files/IRENA/Agency/Publication/2024/Sep/IRENA_Renewable_power_generation_costs_in_2023.pdf (accessed on 3 March 2025).
29. Navidi, W.C. *Statistics for Engineers and Scientists*, 5th ed.; McGraw-Hill Education: New York, NY, USA, 2020.